Applied Ocean Research 28 (2006) 113–119

Applied Ocean Research

Water wave scattering by bottom undulations in the presence of a thin partially immersed barrier

B.N. Mandal*, Rupanwita Gayen

Physics and Applied Mathematics Unit, Indian Statistical Institute, 203, B.T. Road, Kolkata - 700 108, India

Received 16 November 2005; accepted 13 June 2006
Available online 10 August 2006

Abstract

The problem of water wave scattering by bottom undulations in the presence of a partially immersed thin vertical barrier is investigated here by employing a simplified perturbation analysis. The first-order reflection and transmission coefficients are obtained in terms of integrals involving the shape function describing the bottom undulations and the solution of the scattering problem involving the barrier present in uniform finite depth water. For sinusoidal undulations of bottom symmetric about the plane of the barrier, the first-order transmission coefficient vanishes identically. The corresponding first-order reflection coefficient is computed numerically and the numerical results are depicted graphically against the wave number. Resonant interaction of the incident wave with the bottom undulations is seen to occur for a particular value of the ratio of the surface wavelength to sinusoidal wavelength. As the depth of the lower edge of the barrier tends to zero, the curve for this reflection coefficient almost coincides with the same for the reflection coefficient for the scattering problem involving sinusoidal bottom undulations only.

Keywords: Water wave scattering; Sinusoidal bottom; Partially immersed plane barrier; First-order reflection coefficient

1. Introduction

Problems involving reflection of surface gravity waves by an irregular bottom have gained considerable interest in the literature on linearised theory of water waves due to their importance in finding the effects of naturally occurring bottom obstacles such as sand ripples on the wave propagation. There exists only one explicit solution for the two-dimensional problem of wave propagation over a particular bottom topography considered by Roseau [11]. For general bedforms, a variety of approximate numerical methods have been devised in the literature. One such method uses conformal mapping by which the undisturbed fluid region with variable bottom is transformed into a uniform strip (e.g. Kreisel [5], Fitz-Gerald [3], Hamilton [4]). Newman [9], Miles [8] and Staziker et al. [12] employed integral equation formulation to study surface wave propagation over variable bottom topography. The first two authors considered a vertical step, the depths on either side of which being constants but unequal, while Staziker et al. [12] considered undulations of arbitrary shape at the bottom connecting two fluid regions of same uniform depth.

One aim of studying this class of problems was to investigate the mechanism of wave-induced mass transport that forms sand ripples of some wavelength. If this wavelength is half that of the incident wave, then these ripples produce strong reflected waves thus providing a model of breakwater to protect the offshore areas. Davies [1] considered the problem of wave reflection by a patch of sinusoidal undulations on an otherwise flat bottom using linear perturbation theory followed by an application of Fourier transform after introducing an artificial frictional term in the free surface condition (to ensure the existence of Fourier transform in the mathematical analysis). He obtained the reflection and transmission coefficients from the behaviour of the velocity field at either infinity, and observed that when the wavelength of the sinusoidal undulations is half that of the incident wave, a significant amount of wave reflection occurs. Davies and Heathershaw [2] confirmed this theoretical result by conducting experiments in a wave tank.

In all the above problems, the bottom irregularity is the only hindrance to the propagation of surface gravity waves. In the present paper, the additional effect of the presence of a thin vertical partially immersed plate on the propagation of surface waves in the presence of an irregular bottom topography is investigated. To solve the corresponding boundary value problem, a perturbation method is employed directly to the governing partial differential equation, the boundary and infinity conditions satisfied by the potential function describing the fluid motion. This procedure produces a series of boundary value problems (BVPs) for potential functions of increasing orders, of which we consider only the first two BVPs, for the *zero-order* and the *first-order* potential functions. The BVP for the zero-order potential function is concerned with the problem of wave scattering by a thin vertical plate partially immersed in water of *uniform* finite depth and we call it as BVPI. This problem has earlier been solved approximately by Losada et al. [6], Mandal and Dolai [7] and Porter and Evans [10]. While Losada et al. [6] utilized a method based on the principle of least squares, Mandal and Dolai [7] and Porter and Evans [10] reduced it to integral equations which are solved by employing Galerkin approximations (single-term and multi-term) and determined very accurate numerical estimates for the reflection and the transmission coefficients. These are in fact the *zero-order* coefficients. The *first-order* potential function satisfies a radiation problem in water of uniform finite depth, which we refer to as BVPII, involving the *first-order* reflection and transmission coefficients in the radiation condition. Analytical expressions for these first-order coefficients are obtained by using Green's integral theorem, in terms of integrals involving the shape function describing the bottom topography and the solution of the BVPI. It may be noted that the solution of the BVPI cannot be derived explicitly. However, the solution can be expressed in terms of expressions involving unknown constants which are determined by using the multi-term Galerkin approximations (cf. Porter and Evans [10]). For obtaining numerical results the bottom topography is taken in the form of patches of sinusoidal ripples symmetric about the plane of the barrier. In this case the first-order transmission coefficient vanishes identically. The first-order reflection coefficient ($|R_1|$) is depicted graphically against the wave number for different values of the barrier depth, ripple numbers and ripple amplitude. As mentioned earlier, if α, defined as the ratio of twice the ripple wavelength to the wavelength of surface water waves, approaches unity, occurrence of large reflection of the incident wave is a common feature in the absence of the barrier. In the presence of the barrier, this phenomenon of occurrence of large reflection is also observed for a value of α somewhat less than unity and the maximum value of $|R_1|$ is also reduced compared to its maximum value in the absence of the barrier. However, the joint effect of the barrier and the irregular bottom topography will always produce stronger reflection. Known numerical results for $|R_1|$ in the absence of the barrier are recovered by choosing a very small depth of the lower edge of the barrier below the free surface compared to the depth of the bottom. It may be noted that a combination of a partially immersed thin vertical plate and an irregular bottom topography will serve as an effective breakwater for coastal protection.

2. Formulation of the problem

We consider water of finite depth having small undulations at the bottom. A Cartesian co-ordinate system is chosen such that the xz-plane coincides with the undisturbed free surface, y-axis being taken vertically downwards into the fluid occupying the region described by $-\infty < x, z < \infty, 0 < y < h + \epsilon c(x)$. Here $c(x)$ is a continuous bounded function describing the shape of the bottom, $c(x) \to 0$ as $|x| \to \infty$ and ϵ is a very small dimensionless parameter giving a measure of smallness of the bottom undulations. Let a thin vertical plate be partially immersed upto a depth a below the mean free surface, and the plate whose position is described by $x = 0, 0 < y < a$, be very long in the z direction so that the problem of ensuing motion due to a surface wave train incident normally on the plate, is two-dimensional and depends on x, y only. The incident wave train propagating from the direction of negative infinity is partially reflected by the plate and the bottom undulations and transmitted through the gap between the plate and the bottom. Assuming linear theory and irrotational motion, the velocity potential describing the fluid motion can be represented as $Re\{\phi^{inc}(x, y)e^{-i\sigma t}\}$ where σ is the circular frequency. Then $\phi(x, y)$ satisfies

$$\nabla^2\phi = 0 \quad \text{in the fluid region,} \tag{2.1}$$

the free surface condition

$$K\phi + \phi_y = 0 \quad \text{on } y = 0, \tag{2.2}$$

where $K = \sigma^2/g$, g being the gravity, the plate condition

$$\phi_x = 0 \quad \text{on } x = 0, 0 < y < a, \tag{2.3}$$

the bottom condition

$$\phi_n = 0 \quad \text{on } y = h + \epsilon c(x) \tag{2.4}$$

n denoting the normal derivative, the edge condition

$$r^{1/2}\nabla\phi \text{ is bounded as } r = \{x^2 + (y - a)^2\}^{1/2} \to 0, \tag{2.5}$$

and the infinity conditions

$$\phi(x, y) \to \begin{cases} (e^{ik_0x} + Re^{-ik_0x})\psi_0(y) & \text{as } x \to -\infty, \\ Te^{ik_0x}\psi_0(y) & \text{as } x \to \infty \end{cases} \tag{2.6}$$

where

$$\psi_0(y) = N_0^{-1/2}\cosh k_0(h - y) \tag{2.7}$$

with

$$N_0 = \frac{2k_0h + \sinh 2k_0h}{4k_0},$$

k_0 being the real positive root of the transcendental equation

$$k\tanh kh = K. \tag{2.8}$$

In (2.6), R and T denote respectively the unknown reflection and transmission coefficients. The main concern here is to find the coefficients approximately.

The bottom condition (2.4) can be expressed approximately as

$$\phi_y - \epsilon \frac{\mathrm{d}}{\mathrm{d}x}\{c(x)\phi_x\} + 0(\epsilon^2) = 0 \quad \text{on } y = h. \tag{2.9}$$

This suggests that a perturbation technique can be employed to solve the BVP described by (2.1)–(2.6) approximately. This is described in the next section.

3. Method of solution

The approximate boundary condition (2.9) suggests that ϕ, R, T can be expanded in terms of ϵ as given by

$$\left.\begin{aligned} &\phi(x, y; \epsilon) = \phi_0 + \epsilon\phi_1 + O(\epsilon^2),\\ &R(\epsilon) = R_0 + \epsilon R_1 + O(\epsilon^2),\\ &T(\epsilon) = T_0 + \epsilon T_1 + O(\epsilon^2). \end{aligned}\right\} \tag{3.1}$$

Substituting the expansions (3.1) in (2.1)–(2.3), (2.5), (2.6) and (2.9) we find after equating the coefficients of ϵ^0 and ϵ from both sides, that the functions $\phi_0(x, y)$ and $\phi_1(x, y)$ satisfy the following BVPs:

BVP-I The function $\phi_0(x, y)$ satisfies

$$\nabla^2\phi_0 = 0, \quad 0 < y < h,$$
$$K\phi_0 + \phi_{0y} = 0, \quad y = 0,$$
$$\phi_{0x} = 0, \quad x = 0, 0 < y < a,$$
$$\phi_{0y} = 0, \quad y = h,$$
$$r^{1/2}\nabla\phi_0 \text{ is bounded as } r \to 0,$$

$$\phi_0(x, y) \to \begin{cases} (\mathrm{e}^{\mathrm{i}k_0x} + R_0\mathrm{e}^{-\mathrm{i}k_0x})\psi_0(y) & \text{as } x \to -\infty \\ T_0\mathrm{e}^{\mathrm{i}k_0x}\psi_0(y) & \text{as } x \to \infty. \end{cases} \tag{3.2}$$

BVP-II The function $\phi_1(x, y)$ satisfies

$$\nabla^2\phi_1 = 0, \quad 0 < y < h,$$
$$K\phi_1 + \phi_{1y} = 0, \quad y = 0,$$
$$\phi_{1x} = 0, \quad x = 0, 0 < y < a,$$
$$\phi_{1y} = \frac{\mathrm{d}}{\mathrm{d}x}\{c(x)\phi_{0x}\}, \quad y = h,$$
$$r^{1/2}\nabla\phi_1 \text{ is bounded as } r \to 0,$$

$$\phi_1(x, y) \to \begin{cases} R_1\mathrm{e}^{-\mathrm{i}k_0x}\psi_0(y) & \text{as } x \to -\infty \\ T_1\mathrm{e}^{\mathrm{i}k_0x}\psi_0(y) & \text{as } x \to \infty. \end{cases} \tag{3.3}$$

It may be noted that the BVP-I corresponds to the problem of water wave scattering by a thin vertical barrier partially immersed in water of *uniform* finite depth h. This has been solved in the literature approximately in the sense that numerical estimates for R_0 and T_0 have been obtained (Losada et al. [6], Mandal and Dolai [7] and Porter and Evans [10]).

The BVP-II is a radiation problem in water of *uniform* finite depth h, in which, the bottom condition involves ϕ_0, the solution of BVP-I. Without solving $\phi_1(x, y)$ explicitly, R_1 and T_1 can be determined in terms of integrals involving the shape function $c(x)$ and $\phi_{0x}(x, h)$. To show this, we apply Green's integral theorem to the functions $\phi_0(x, y)$ and $\phi_1(x, y)$ in the region bounded by the lines

$y = 0, 0 < x \le X$; $x = X, 0 \le y \le h$; $y = h, -X \le x \le X$;
$x = -X, 0 \le y \le h$;
$y = 0, -X < x < 0$; $x = 0+, 0 \le y \le a$; $x = 0-, 0 \le y \le a$

where X is large and positive, and ultimately makes X to tend to infinity. This produces

$$2\mathrm{i}k_0R_1 = \int_{-\infty}^{\infty} c(x)\phi_{0x}^2(x, h)\mathrm{d}x. \tag{3.4}$$

Similarly, applying Green's integral theorem to $\chi_0(x, y) = \phi_0(-x, y)$ and $\phi_1(x, y)$ in the same region and making $X \to \infty$, we find

$$2\mathrm{i}k_0T_1 = -\int_{-\infty}^{\infty} c(x)\phi_{0x}(x, h)\phi_{0x}(-x, h)\mathrm{d}x. \tag{3.5}$$

Thus both R_1 and T_1 are derived in terms of integrals involving the shape function $c(x)$ and the zero-order potential function $\phi_0(x, y)$. Unfortunately $\phi_0(x, y)$ cannot be obtained analytically. However it can be expressed as

$$\phi_0(x, y) = \begin{cases} (\mathrm{e}^{\mathrm{i}k_0x} + R_0\mathrm{e}^{-\mathrm{i}k_0x})\psi_0(y) + \displaystyle\sum_{n=1}^{\infty} A_n\mathrm{e}^{k_nx}\psi_n(y), \\ \qquad x < 0, \\ T_0\mathrm{e}^{\mathrm{i}k_0x}\psi_0(y) + \displaystyle\sum_{n=1}^{\infty} B_n\mathrm{e}^{-k_nx}\psi_n(y), \\ \qquad x > 0 \end{cases} \tag{3.6}$$

where $\pm\mathrm{i}k_n$ $(n = 1, 2, \ldots)$ are the purely imaginary roots of (2.8), A_n, B_n $(n = 1, 2, \ldots)$ are unknown constants,

$$\psi_n(y) = N_n^{-1/2}\cos k_n(h - y)$$

with

$$N_n = \frac{2k_nh + \sin 2k_nh}{4k_n}. \tag{3.7}$$

It can be shown that $R_0 = 1 - T_0$ and $A_n = -B_n (n = 1, 2, \ldots)$. R_0 (and hence T_0) can be estimated numerically by using multi-term Galerkin approximations employed by Porter and Evans [10]. The same method can be used to estimate numerically the constants $A_n (n = 1, 2, \ldots)$. The details are given in the Appendix. Thus R_1 and T_1 can be computed numerically once the shape function $c(x)$ is known. Here we consider sinusoidal undulations at the bottom so that $c(x)$ can be taken in the form

$$c(x) = \begin{cases} c_0\sin\lambda x, & -\dfrac{m\pi}{\lambda} \le x \le \dfrac{m\pi}{\lambda} \\ 0, & \text{otherwise} \end{cases} \tag{3.8}$$

where m is a positive integer. Thus there exists m number of sinusoidal ripples at the bottom with wave number λ. In this case T_1 vanishes identically, and R_1 is given by

$$R_1 = \frac{c_0k_0(R_0 - 1)}{2N_0}\left\{\frac{\sin(\lambda - 2k_0)l}{\lambda - 2k_0} - \frac{\sin(\lambda + 2k_0)l}{\lambda + 2k_0}\right\}$$
$$+ \frac{\mathrm{i}c_0k_0R_0}{2N_0}\left\{\frac{2(1 - \cos\lambda l)}{\lambda} - \frac{2\lambda}{\lambda^2 - 4k_0^2}\right.$$

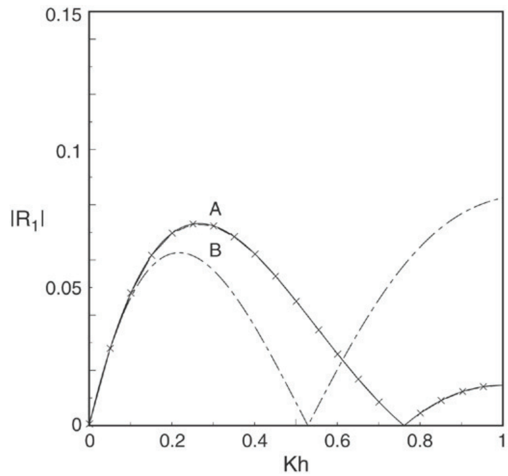

Fig. 1. $|R_1|$ for different plate-length with $c_0/h = 0.1$, $m = 1$: $a/h = 0.001$ (A), 0.5 (B) Crosses denote data for $|R_1|$ when there is no plate.

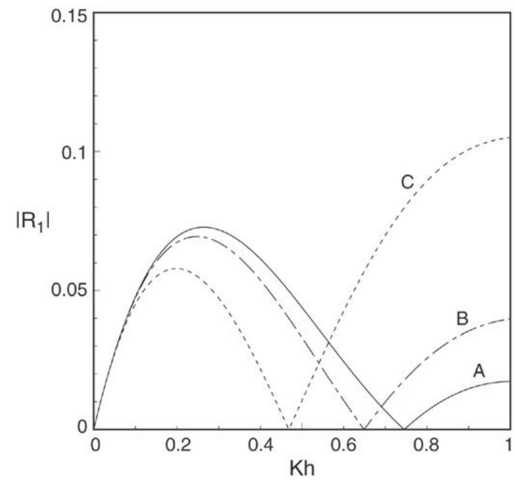

Fig. 2. $|R_1|$ for different plate-length with $c_0/h = 0.1$, $m = 1$: $a/h = 0.1$ (A), 0.3 (B), 0.6 (C).

$$
\begin{aligned}
&+\frac{\cos(\lambda-2k_0)l}{\lambda-2k_0}+\frac{\cos(\lambda+2k_0)l}{\lambda+2k_0}\Bigg\}\\
&+\frac{\mathrm{i}c_0}{N_0^{1/2}}\sum_{n=1}^{\infty}\Bigg[\frac{k_n}{k_n^2+(\lambda-k_0)^2}-\frac{k_n}{k_n^2+(\lambda+k_0)^2}\\
&+\Bigg\{\frac{(\lambda-k_0)\sin(\lambda-k_0)l-k_n\cos(\lambda-k_0)l}{k_n^2+(\lambda-k_0)^2}\\
&-\frac{(\lambda+k_0)\sin(\lambda+k_0)l-k_n\cos(\lambda+k_0)l}{k_n^2+(\lambda+k_0)^2}\Bigg\}\mathrm{e}^{-k_nl}\Bigg]\\
&\times\frac{k_nA_n}{N_n^{1/2}}. \qquad (3.9)
\end{aligned}
$$

4. Numerical results

For numerical computation of R_1, we need to evaluate R_0 and the constants A_n $(n = 1, 2, \ldots)$ associated with the solution $\phi_0(x, y)$ of the BVPI. As mentioned above, these are evaluated numerically by using multi-term Galerkin approximations. Only a few terms (at most three) in these approximations are sufficient to produce fairly accurate numerical estimates for R_1 (real and imaginary parts).

In our numerical computations the value of λh is chosen to be unity for Figs. 1–5. The Figs. 1 and 2 depict $|R_1|$ against the wave number Kh for different values of a/h and a single ripple ($m = 1$) and $c_0/h = 0.1$. From these two figures it is observed that $|R_1|$, regarded as a function of Kh is oscillatory in nature. The zeros of $|R_1|$ are shifted towards the left as the depth of the lower edge of the barrier increases. The crosses in Fig. 1 represent the data for $|R_1|$ in the absence of the barrier (for which case $R_0 \equiv 0$). These crosses almost lie on the curve for $|R_1|$ for a very small depth of the lower edge of the barrier ($a/h = 0.001$). This is obviously expected and also confirms the correctness of the numerical results.

The Fig. 3 depicts $|R_1|$ against Kh for different values of m, the number of ripples and fixed a/h and c_0/h. As m increases, $|R_1|$ increases, becomes more oscillatory and the number of zeros also increases. This is due to multiple interaction of the incident wave between the ripple tops, the barrier and the free surface.

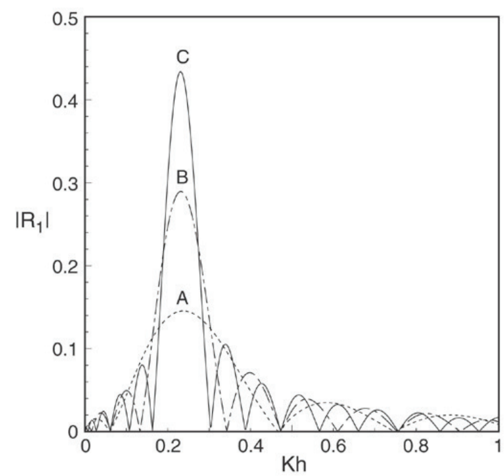

Fig. 3. $|R_1|$ for different number of ripples with $a/h = 0.3$, $c_0/h = 0.1$: $m = 2$ (A), 4 (B), 6 (C).

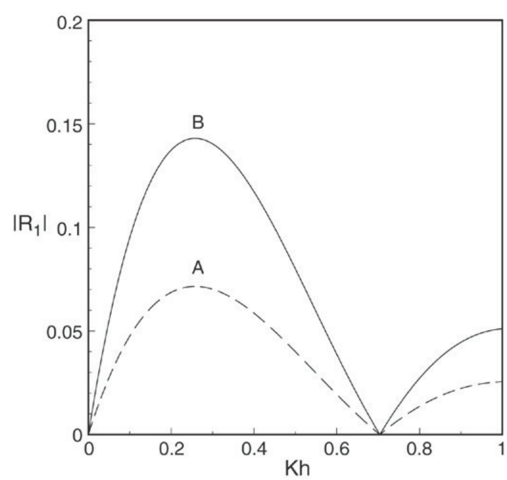

Fig. 4. $|R_1|$ for different ripple amplitude with $a/h = 0.2$, $m = 1$: $c_0/h = 0.1$ (A), 0.2 (B).

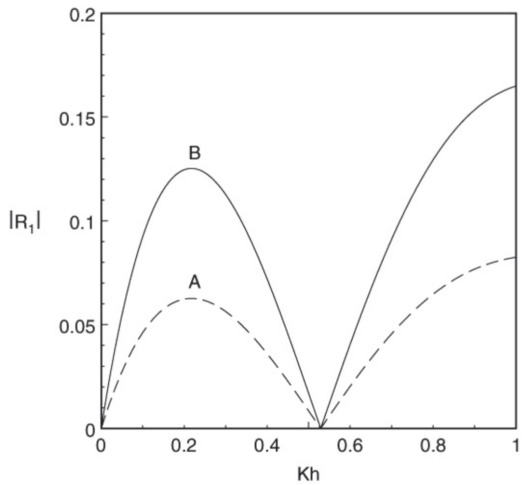

Fig. 5. $|R_1|$ for different ripple amplitude with $a/h = 0.5$, $m = 1$: $c_0/h = 0.1$ (A), 0.2 (B).

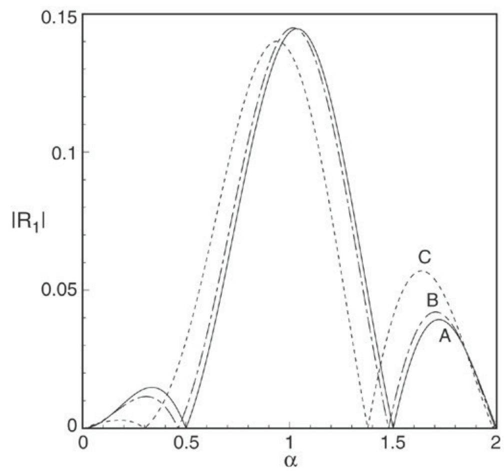

Fig. 6. $|R_1|$ against α with $c_0/h = 0.1$, $m = 2$, $Kh = 0.25$: $a/h = 0$ (A), 0.4 (B), 0.8 (C).

The Figs. 4 and 5 show the effect of c_0/h (non-dimensional ripple amplitude) on $|R_1|$. As c_0/h increases, $|R_1|$ also increases, whatever be the plate-length, and the zeros of $|R_1|$ remain unchanged with the change in c_0/h, but shift towards the left as a/h increases.

It is known that in the absence of the barrier, $|R_1|$ has peak value when $\alpha = \frac{2k_0}{\lambda} \approx 1$. A similar feature of $|R_1|$ is also evident in the Figs. 6 and 7 depicting $|R_1|$ against α for fixed c_0/h (=0.1), m(=2), $Kh = 0.25$ (in Fig. 6), $Kh = 1.5$ (in Fig. 7), in which the curve A represents the case of absence of barrier. However, the value of α for which $|R_1|$ attains its peak, is somewhat less than unity and the peak values are also reduced as a/h increases. These features are prominent for large wave numbers.

5. Conclusion

The problem of water wave scattering by a variable bottom in the presence of a thin vertical surface piercing barrier is investigated by employing a simplified perturbation analysis. The first-order reflection and transmission coefficients R_1

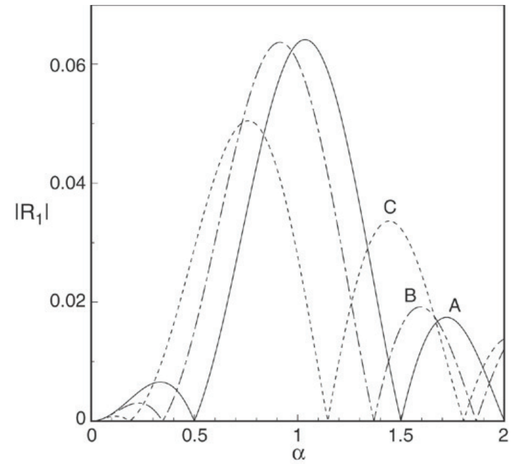

Fig. 7. $|R_1|$ against α with $c_0/h = 0.1$, $m = 2$, $Kh = 1.5$: $a/h = 0$ (A), 0.4 (B), 0.8 (C).

and T_1 are determined in terms of integrals involving the shape function describing the bottom and the solution of the corresponding scattering problem for *uniform* finite depth water. For the particular case of a patch of sinusoidal ripples at the bottom, R_1 is depicted in a number of figures. As a function of the wave number Kh, R_1 is oscillatory in nature due to multiple interaction of the incident wave with the bottom undulations, the lower edge of the plate and the free surface. Somewhat large values of R_1 are found to occur for some particular value of the ratio of the incident wavelength and the bottom wavelength. Also the overall values of R_1 are somewhat decreased due to the presence of the barrier compared to the case when there is no barrier.

A similar method can be used to investigate the water wave scattering problems involving a thin vertical plate or a bottom standing submerged plate present in water of variable depth.

Acknowledgements

This work is supported by CSIR, New Delhi (through a research project to BNM) and NBHM, Mumbai (through a post doctoral fellowship to RG).

Appendix

A brief outline for estimating numerically the constants R_0 and $A_n (n = 1, 2, \ldots)$ is given here.

Let

$$f(y) = \phi_0(+0, y) - \phi_0(-0, y) \quad \text{and}$$

$$g(y) = \frac{\partial \phi_0}{\partial x}(0, y), \quad 0 < y < h. \tag{A1}$$

Then

$$f(y) = 0 \quad \text{for } a < y < h \quad \text{and}$$

$$g(y) = 0 \quad \text{for } 0 < y < a.$$

Using (3.6) in the definition of $g(y)$, we have

$$g(y) = \mathrm{i}k_0(1 - R_0)\psi_0(y) + \sum_{n=1}^{\infty} k_n A_n \psi_n(y), \quad 0 < y < h$$

and

$$g(y) = \mathrm{i}k_0 T_0 \psi_0(y) - \sum_{n=1}^{\infty} k_n B_n \psi_n(y), \quad 0 < y < h.$$

Use of Havelock inversion theorem produces

$$\left.\begin{aligned} \mathrm{i}k_0(1 - R_0) = \mathrm{i}k_0 T_0 &= \int_a^h g(y)\psi_0(y)\mathrm{d}y, \\ k_n A_n = -k_n B_n &= \int_a^h g(y)\psi_n(y)\mathrm{d}y. \end{aligned}\right\} \tag{A2}$$

Again using (3.6) in the definition of $f(y)$, we similarly find that

$$\begin{aligned} 2R_0 &= -\int_0^a f(y)\psi_0(y)\mathrm{d}y, \\ 2A_n &= -\int_0^a f(y)\psi_n(y)\mathrm{d}y. \end{aligned} \tag{A3}$$

If we define

$$F(y) = \frac{f(y)}{2\mathrm{i}k_0(1 - R_0)}, \quad 0 < y < a, \quad \text{and}$$
$$G(y) = -\frac{g(y)}{R_0}, \quad a < y < h, \tag{A4}$$

then $F(y)$ and $G(y)$ satisfy the integral equations

$$\int_0^a F(t)\mathcal{K}_F(y, t)\mathrm{d}t = \psi_0(y), \quad 0 < y < a \tag{A5}$$

and

$$\int_a^h G(t)\mathcal{K}_G(y, t)\mathrm{d}t = \psi_0(y), \quad a < y < h \tag{A6}$$

where

$$\mathcal{K}_F(y, t) = \sum_{n=1}^{\infty} k_n \psi_n(y)\psi_n(t), \quad 0 < y, t < a \tag{A7}$$

and

$$\mathcal{K}_G(y, t) = \sum_{n=1}^{\infty} \frac{\psi_n(y)\psi_n(t)}{k_n}, \quad a < y, t < h, \tag{A8}$$

together with

$$\int_0^a F(y)\psi_0(y)\mathrm{d}y = \frac{1}{C} \quad \text{and}$$
$$\int_a^h G(y)\psi_0(y)\mathrm{d}y = C \tag{A9}$$

where

$$C = \mathrm{i}k_0\left(1 - \frac{1}{R_0}\right). \tag{A10}$$

It may be noted that the functions $F(y)$, $G(y)$ and the constant C are all real. The integral Eqs. (A5) and (A6) are solved by multi-term Galerkin approximations (cf. Porter and Evans [10]) given by

$$F(y) = \sum_{n=1}^{\infty} a_n f_n(y), \quad 0 < y < a \tag{A11}$$

and

$$G(y) = \sum_{n=1}^{\infty} b_n g_n(y), \quad a < y < h \tag{A12}$$

where

$$f_n(y) = \frac{\mathrm{d}}{\mathrm{d}y}\left[\mathrm{e}^{-Ky}\int_y^a \widehat{f}_n(u)\mathrm{e}^{Ku}\mathrm{d}u\right], \quad 0 < y < a$$

with

$$\widehat{f}_n(y) = \frac{2(-1)^n}{\pi(2n+1)ah}(a^2 - y^2)^{1/2}U_{2n}\left(\frac{y}{a}\right) \tag{A13}$$

and

$$g_n(y) = \frac{2(-1)^n}{\pi\{(h-a)^2 - (h-y)^2\}^{1/2}}T_{2n}\left(\frac{h-y}{h-a}\right),$$
$$a < y < h, \tag{A14}$$

U_{2n} and T_{2n} being the Chebyshev polynomials of second and first kinds respectively. The unknown coefficients a_n, b_n $(n = 0, 1, \ldots, N)$ are obtained by using the systems of linear equations

$$\sum_{n=0}^{\infty} a_n \mathcal{K}_{mn}^F = F_m, \quad m = 0, 1, \ldots, N,$$

and

$$\sum_{n=0}^{\infty} b_n \mathcal{K}_{mn}^G = G_m, \quad m = 0, 1, \ldots, N \tag{A15}$$

where

$$\mathcal{K}_{mn}^F = \sum_{l=0}^{\infty} k_l \left(\int_0^a \psi_l(y) f_n(y)\mathrm{d}y\right)\left(\int_0^a \psi_l(t) f_m(t)\mathrm{d}t\right),$$
$$F_m = \int_0^a \psi_0(y) f_m(y)\mathrm{d}y, \tag{A16}$$

and

$$\mathcal{K}_{mn}^G = \sum_{l=0}^{\infty} \frac{1}{k_l}\left(\int_a^h \psi_l(y) g_n(y)\mathrm{d}y\right)\left(\int_a^h \psi_l(t) g_m(t)\mathrm{d}t\right),$$
$$G_m = \int_a^h \psi_0(y) g_m(y)\mathrm{d}y. \tag{A17}$$

Once a_n, b_n $(n = 0, 1, \ldots, N)$ are derived, the real constant C can be determined by using any one of the equations in (A9) after substituting from (A11) or (A12). R_0 then can be found by using (A10).

To find the constants A_n, we use either the second relation in (A2) or in (A3). Noting the relations in (A4) and the multi-term expansions (A11) or (A12), A_n is ultimately approximated as

$$A_n = -\mathrm{i}k_0(1 - R_0)\sum_{l=0}^{N} a_l \int_0^a \psi_n(y) f_l(y)\mathrm{d}y$$

or

$$A_n = -R_0 \sum_{l=0}^{N} b_l \int_a^h \psi_n(y) g_l(y) \mathrm{d}y. \tag{A18}$$

In the numerical computations for R_1, both the sets of multi-term Galerkin approximations for $F(y)$ and $G(y)$ have been used. Almost the same numerical results for R_1 are obtained.

References

[1] Davies AG. The reflection of wave energy by undulations on the seabed. Dyn Atmos Oceans 1982;6:121–3.

[2] Davies AG, Heathershaw AD. Surface wave propagation over sinusoidally varying topography. J Fluid Mech 1984;144:419–43.

[3] Fitz-Gerald GF. The reflexion of plane gravity waves travelling in water of variable depth. Phil Trans Roy Soc Lond 1976;34:49–89.

[4] Hamilton J. Differential equations for long-period gravity waves on fluid of rapidly varying depth. J Fluid Mech 1977;83:289–310.

[5] Kreisel G. Surface waves. Quart Appl Math 1949;7:21–44.

[6] Losada IJ, Losada MA, Roldan AJ. Propagation of oblique incident wave past rigid vertical thin barriers. Appl Ocean Res 1992;14:191–9.

[7] Mandal BN, Dolai DP. Oblique water wave diffraction by thin vertical barriers in water of uniform finite depth. Appl Ocean Res 1994;16:195–203.

[8] Miles JW. Surface wave scattering matrix for a shelf. J Fluid Mech 1967;28:755–67.

[9] Newman JN. Propagation of water waves over an infinite step. J Fluid Mech 1965;23:399–415.

[10] Porter R, Evans DV. Complementary approximations to waves scattering by vertical barriers. J Fluid Mech 1995;294:160–86.

[11] Roseau M. Asymptotic wave theory. North Holland; 1976. p. 311–47.

[12] Staziker DJ, Porter D, Stirling DSG. The scattering of surface waves by local bed elevations. Appl Ocean Res 1996;18:283–91.